ASME Paper Title: Analysis of large-amplitude oscillations in triple-well non-natural systems

Authors: Lai, S. K., Yang, X., & Gao, F. B.

ASME Journal Title: Journal of Computational and Nonlinear Dynamics

Volume/Issue 14(9) Date of Publication (VOR* Online) July 15, 2019

ASME Digital Collection URL: https://asmedigitalcollection.asme.org/computationalnonlinear/article/14/9/091002/ of-Large-Amplitude-Oscillations-in-Triple

DOI: https://doi.org/10.1115/1.4043833

Analysis for Large-amplitude Oscillation of Triple-well Non-natural Systems

S.K. Lai[1,2,*], X. Yang[1], F.B. Gao[3,4]

[1] Department of Civil and Environmental Engineering, The Hong Kong Polytechnic University, Hung Hom, Kowloon, Hong Kong, P.R. China

[2] The Hong Kong Polytechnic University Shenzhen Research Institute, Nanshan, Shenzhen, P.R. China

[3] School of Mathematical Science, Yangzhou University, Yangzhou, 225002, P.R. China

[4] Departament de Matemàtiques, Universitat Autònoma de Barcelona, 08193 Bellaterra, Barcelona, Spain

Abstract

In this paper, the large-amplitude oscillation of a triple-well non-natural system, covering both qualitative and quantitative analysis, is investigated. The nonlinear system is governed by a quadratic velocity term and an odd-parity restoring force having cubic and quintic nonlinearities. Many mathematical models in mechanical and structural engineering applications can give rise to this nonlinear problem. In terms of qualitative analysis, the equilibrium points and its trajectories due to the change of the governing parameters are studied. It is interesting that there exist heteroclinic and homoclinic orbits under different equilibrium states. By adjusting the parameter values, the dynamic behaviour of this conservative system is shifted accordingly. As exact solutions for this problem expressed in terms of an integral form must be solved numerically, an analytical approximation method can be used to construct accurate solutions to the oscillation around the stable equilibrium points of this system. This method is based on the harmonic balance method incorporated with Newton's method, in which a series of linear algebraic equations can be derived to replace coupled and complicated nonlinear algebraic equations. According to this harmonic balance-based approach, only the use of Fourier series expansions of known functions is required. Accurate analytical approximate solutions can be derived using lower-order harmonic balance procedures. The proposed analytical method can offer good agreement with the corresponding numerical results for the whole range of oscillation amplitudes.

Keywords: Non-natural system, Triple-well, Analytical approximations, Equilibrium states.

*Corresponding author. *E-mail address:* sk.lai@polyu.edu.hk

1. Motivation

Consider a nonlinear problem

$$E\left(x\right)\frac{d^2x}{dt^2}+F\left(x\right)\left(\frac{dx}{dt}\right)^2+G\left(x\right)=0 \tag{1}$$

with the following initial conditions

$$x(0)=A, \qquad \frac{dx}{dt}(0)=0 \tag{2}$$

where $E(x)=1+\alpha_1 x^2$, $F(x)=\alpha_1 x$ and $G(x)=\alpha_2 x+\alpha_3 x^3+\alpha_4 x^5$. x and t are dimensionless displacement and time variables, respectively. The governing parameters α_1, α_2, α_3 and α_4 in the functions $E\left(x\right)$, $F\left(x\right)$ and $G\left(x\right)$ are real constants. This system is governed by a quadratic dependence term on the velocity [1] and an odd-parity restoring force having cubic-quintic nonlinearities.

Integrating Eq. (1) yields

$$T+V=E \tag{3}$$

in which

$$T=\frac{1}{2}\left(1+\alpha_1 x^2\right)y^2 \quad \text{and} \quad V=\frac{1}{2}\alpha_2 x^2+\frac{1}{4}\alpha_3 x^4+\frac{1}{6}\alpha_4 x^6 \tag{4}$$

where $y=dx/dt$. In Eq. (3), the first term on the left-hand side is the kinetic energy and the second one is the potential energy. The constant value E is the total energy level that can be determined by the initial conditions in Eq. (2). Because the kinetic energy of this system is not purely a quadratic function of the velocity, it is also called as a non-natural system [2, 3].

Although there is a quadratic dependence term on the velocity in Eq. (1), the nonlinear problem is still a conservative system. A simple argument to show the existence of periodic motions with the presence of a quadratic dependence term on the velocity in dynamical problems is provided below [4]. Consider the following simple oscillator

$$\frac{d^2x}{dt^2}+\varepsilon_1\left(\frac{dx}{dt}\right)^2+\varepsilon_2 x=0 \tag{5}$$

where ε_1 and ε_2 are real parameters. Multiplying Eq. (5) by $y\left(\equiv dx/dt\right)$ and integrating from 0 to t yield

$$\left[y^2+\varepsilon_2 x^2\right]_0^t=-2\varepsilon_1\int_0^t y^3 dt \tag{6}$$

If a periodic mode exists and t is the period, then the left-hand side of Eq. (6) is equal to zero. For a cubic power on the right-hand side, it is plausible that the integral may vanish to form a close trajectory in the phase-space plane (x, y). However, the integral may not vanish for a second or even power of y. This is consistent with the fact that a classical damped harmonic oscillator (e.g., $d^2x/dt^2 + c\left(dx/dt\right) + \omega_0^2 x = 0$) does not have a periodic oscillation mode.

Many mathematical models in mechanical and structural engineering applications can give rise to the nonlinear problem in Eq. (1). In the literature, one practical example can be found is the large-amplitude vibration of stringer cylindrical shells [5−7], in which the studied parameters are restricted to all positive values $\left(\alpha_i > 0,\ \ i = 1-4\right)$. Stringer cylindrical shells are tube-shaped structures with supporting ribs situated along the length uniformly with a constant distance between them. In this case, there is only a single potential well in the system. It is commonly known that there is always an inherent mechanism to provoke bifurcations and instabilities that can induce unpredictable responses in nonlinear dynamics. Generally, a local bifurcation would occur when there is a change of governing parameters and initial conditions, leading to the instability of equilibrium states. Hence, various combinations of the governing parameters in Eq. (1) will generate diverse responses. It is found that there exist both heteroclinic and homoclinic orbits under various equilibrium states.

Indeed, many other examples in various engineering and physical models where Eq. (1) arises are:

- Absence of quadratic velocity and quintic nonlinearity (i.e., $\alpha_1 = 0$, $\alpha_2 \neq 0$, $\alpha_3 \neq 0$ and $\alpha_4 = 0$): this is a simple Duffing equation that can model the nonlinear vibration of beams, panels and fluid-conveying pipes [8−10], the dynamic buckling problem of a drillstring in a horizontal well [11] and the nonlinear cantilevered piezoelectric energy harvesters [12–14];
- Absence of quadratic velocity (i.e., $\alpha_1 = 0$, $\alpha_2 \neq 0$, $\alpha_3 \neq 0$ and $\alpha_4 \neq 0$): the problem becomes a cubic-quintic Duffing equation that can model the nonlinear dynamics of a slender elastica [15], the large-amplitude vibration of a restrained uniform beam carrying intermediate lumped mass [16] and a rotating pendulum system as vibration absorbers and fly-ball governors [17];
- Absence of quintic nonlinearity (i.e., $\alpha_1 \neq 0$, $\alpha_2 \neq 0$, $\alpha_3 \neq 0$ and $\alpha_4 = 0$): the equation can be used to model the nonlinear dynamics of cantilever beams, flexible rotating beams and tapered beams [18−20]; and

- Absence of cubic and quintic nonlinear terms (i.e., $\alpha_1 \neq 0$, $\alpha_2 \neq 0$, $\alpha_3 = 0$ and $\alpha_4 = 0$): the equation can be used to model a physical particle on a rotating parabola [3, 21] and a non-polynomial oscillator [22].

Although some special cases of Eq. (1) have been treated in the literature, the overall version of Eq. (1) has not yet been investigated in detail. In Eq. (1), the pattern of equilibrium points is not related to the value of the parameter α_1, as there are no practical applications for $\alpha_1 < 0$. We only consider $\alpha_1 > 0$, $\alpha_2 \neq 0$, $\alpha_3 \neq 0$ and $\alpha_4 \neq 0$ in Eq. (1), including negative linear stiffness and cubic and quintic nonlinearities. In this study, a qualitative analysis is employed to discuss the pattern of equilibrium points. The nature of each equilibrium state is determined due to the influence of the governing parameters. Besides, a quantitative analysis is presented to construct analytical approximate solutions for periodic motions around each stable equilibrium point by means of the Newton Harmonic Balance (NHB) method [23, 24]. This approach has been successfully used to derive accurate approximate solutions for various strongly nonlinear problems in structural and mechanical engineering [11, 25–28]. Making use of the NHB method, a set of linear algebraic equations can be derived to replace coupled and complicated nonlinear algebraic equations that are resulted from the classical harmonic balance method. Only the use of Fourier series expansions of known functions is thus required. Several cases of Eq. (1) with different parameters are presented to illustrate the accuracy and effectiveness of the proposed method. Both qualitative and quantitative studies presented herein can establish a firm understanding of the dynamical characteristics of this system in practical use.

2. Qualitative analysis

This section aims to classify the nonlinear system in terms of their equilibria and stabilities and to provide solutions for various classifications of the system.

Consider the following equation

$$\frac{dV(x_i)}{dx} = \alpha_2 x_i + \alpha_3 x_i^3 + \alpha_4 x_i^5 = 0 \tag{7}$$

and the stability of the equilibrium points can be determined by examining

$$\frac{d^2V(x_i)}{dx^2} = \alpha_2 + 3\alpha_3 x_i^2 + 5\alpha_4 x_i^4 \tag{8}$$

at the equilibrium points x_i. The pattern of the roots of Eq. (7) varies with different values of the parameters. Table 1 lists all the cases to be considered according to different values of the parameters. The number of equilibrium points and the orbital characteristics around centers are also determined. Note that these cases correspond to three patterns of the roots, i.e., 1, 3 or 5 equilibrium points.

For cases that have only one equilibrium point x_1, there are two situations. In cases 1 and 3, the system has a minimum potential energy level at x_1 where is a center. While in case 8, the system reaches a maximum potential energy level at x_1 where is a saddle point. The possible trajectories for these two cases are shown in Fig. 1.

On the other hand, there exist three equilibrium points x_1, x_2 and x_3 in the system and there are four situations. In cases 2 and 7, the potential energy levels have a local maximum at x_1 and two minima at x_2 and x_3. Hence, x_1 is a saddle point while x_2 and x_3 are centers. In cases 6 and 11, the potential energy levels have a local minimum at x_1 and two maxima at x_2 and x_3. Hence, x_1 now becomes a center and x_2 and x_3 are saddle points. In case 4, the potential energy level has a local minimum at x_1, and x_2 and x_3 are inflection points. Hence, x_1 is a center, and x_2 and x_3 are degenarate singular points. In case 9, the potential energy level has a local maximum value at x_1, and x_2 and x_3 are inflection points. Hence, x_1 is a saddle point, and x_2 and x_3 are degenarate singular points. The possible trajectories are presented in Fig. 2.

There are still two cases that possess five equilibrium points. In case 5, the system arrives its minimum potential energy levels at x_1, x_4 and x_5, and the maximum potential energy levels are at x_2 and x_3. Hence x_1, x_4 and x_5 are centers, and x_2 and x_3 are saddle points. In case 10, the system arrives its minimum potential energy levels at x_2 and x_3, and the maximum potential energy levels at x_1, x_4 and x_5. In this case, x_2 and x_3 are centers, and x_1, x_4 and x_5 become saddle points. The possible trajectories are plotted in Fig. 3.

To further investigate the effect of various parameters (α_1, α_2 and α_3) on the pattern of the roots in Eq. (7), two bifurcation diagrams are plotted in Figs. 4 and 5. Figure 4 presents the relationship between the negative linear stiffness (α_2) and the cubic nonlinear term (α_3), and Fig. 5 shows the variation of the quadratic velocity term (α_1) and the cubic nonlinear term (α_3). In these two figures, we observe that a bifurcation of the system occurs when α_3 tends to become a negetive value.

According to the qualitative analysis for Eq. (1), the periodic motion of the non-natural system only occurs around centers, which depends on the parameter values and the initial amplitudes. In cases 1 and 3, the system oscillates periodically between a symmetric bound $[-A, A]$ and $0 < A < +\infty$. In cases 2 and 7, a periodic oscillation occurs around the stable equilibrium points x_2 (or x_3) and it is asymmetric about the equilibrium points. The oscillation amplitude A is subject to the region $0 < A < K$ ($-K < A < 0$), where K is calculated by

$$K = \sqrt{-\frac{3\alpha_3}{4\alpha_4} + \frac{\sqrt{3(3\alpha_3^{\ 2} - 16\alpha_2\alpha_4)}}{4\alpha_4}} \tag{9}$$

In cases 6 and 11, the presence of periodic motions will occur around the stable equilibrium point x_1 only, which is symmetric about this point and the oscillation amplitude should satisfy $0 < A < x_2$. In case 4, the system oscillates periodically around center x_1 between a symmetric bound $[-A, A]$ and $0 < A < x_2$. In case 5, the oscillation of the system may occur around the stable equilibrium point x_1 and it is symmetric about this point. The oscillation amplitude A is bounded by $0 < A < x_2$. Besides, the oscillation may also occur around the equilibrium point x_4 (or x_5) and it is asymmetric in nature. The oscillation amplitude should satisfy $x_2 < A < L$ (or $-L < A < x_3$), where L is given by

$$L = \sqrt{-\frac{\alpha_3}{2\alpha_4} + \frac{\sqrt{\alpha_3^{\ 2} - 4\alpha_2\alpha_4}}{4\alpha_4} + \frac{1}{4\alpha_4^{\ 2}}\left(\sqrt{8\alpha_3^{\ 2}\alpha_4^{\ 2} - 32\alpha_2\alpha_4^{\ 3} + \alpha_4^{\ 2}(\alpha_3^{\ 2} - 4\alpha_2\alpha_4)}\right)} \tag{10}$$

In case 10, the oscillation occurs around the stable equilibrium point x_2 (or x_3), and it is asymmetric in nature. If $V(x_1) \le V(x_4)$, the oscillation amplitude should satisfy $0 < A < K$ ($-K < A < 0$). While for $V(x_1) > V(x_4)$, the oscillation amplitude should satisfy $M < A < x_4$ (or $x_5 < A < -M$), in which M is defined as

$$M = \sqrt{-\frac{\alpha_3}{2\alpha_4} + \frac{\sqrt{\alpha_3^{\ 2} - 4\alpha_2\alpha_4}}{4\alpha_4} + \frac{1}{4\alpha_4^{\ 2}}\left(\sqrt{8\alpha_3^{\ 2}\alpha_4^{\ 2} - 32\alpha_2\alpha_4^{\ 3} + \alpha_4^{\ 2}(\alpha_3^{\ 2} - 4\alpha_2\alpha_4)}\right)} \tag{11}$$

In the subsequent section, a quantitative analysis for the nonlinear system (1) will be presented.

3. Quantitative analysis

In this section, the NHB method is used to construct analytical approximate solutions to the periodic motion of Eq. (1). As discussed in section 2, there are two types of periodic motions:

the first one is a symmetric oscillation with the stable equilibrium point x_1, and the second one is an asymmetric oscillation with the stable equilibrium points x_2 (x_3) or x_4 (x_5). The solution procedures of this approach are described here.

3.1 Analytical approximations for symmetric oscillations

The system (1) with odd nonlinearity can be directly solved by the NHB method. The procedures of this approach are briefly given in this section for easy reference. Details can be referred to Refs. [23–26]. By defining a new independent variable $\tau = \sqrt{\Omega} t$, Eq. (1) can be expressed as

$$\Omega\left[E(x)\ddot{x} + F(x)\dot{x}^2\right] + G(x) = 0 \tag{12}$$

and the initial conditions are

$$x(0) = A, \quad \dot{x}(0) = 0 \tag{13}$$

where a dot of x denotes differentiation with respect to τ.

Applying the Newton's procedure, the displacement $x(\tau)$ and the square of frequency Ω are written as

$$x(\tau) = x_{a1}(\tau) + \Delta x_{a1}(\tau) \tag{14}$$

$$\Omega = \Omega_{a1} + \Delta\Omega_{a1} \tag{15}$$

in which $\Delta x_{a1}(\tau)$ and $\Delta\Omega_{a1}$ are small increments of $x_{a1}(\tau)$ and Ω_{a1}, respectively. Substituting Eqs. (14) and (15) into Eq. (12), we have

$$\begin{aligned}&(\Omega_{a1} + \Delta\Omega_{a1})\left[E\left(x_{a1} + \Delta x_{a1}\right)(\ddot{x}_{a1} + \Delta\ddot{x}_{a1}) + F\left(x_{a1} + \Delta x_{a1}\right)(\dot{x}_{a1} + \Delta\dot{x}_{a1})^2\right] \\ &+G\left(x_{a1} + \Delta x_{a1}\right) = 0\end{aligned} \tag{16}$$

Further linearizing Eq. (16) with respect to the correction terms $\Delta x_1(\tau)$ and $\Delta\Omega_1$ leads to

$$\begin{aligned}&\Omega_{a1}\left[E(x_{a1})\ddot{x}_{a1} + F(x_{a1})\dot{x}_{a1}^2\right] + G\left(x_{a1}\right) + E(x_{a1})(\Omega_{a1}\Delta\ddot{x}_{a1} + \Delta\Omega_{a1}\ddot{x}_{a1}) + \\ &F\left(x_{a1}\right)\dot{x}_{a1}(2\Omega_{a1}\Delta\dot{x}_{a1} + \Delta\Omega_{a1}\dot{x}_{a1}) + \Omega_{a1}\left[E_x(x_{a1})\ddot{x}_{a1} + F_x(x_{a1})\dot{x}_{a1}^2\right]\Delta x_{a1} + \\ &G_x\left(x_{a1}\right)\Delta x_{a1} = 0\end{aligned} \tag{17}$$

where the subscript x denote differentiation with respect to x. Making use of the Fourier series expansions gives [21]

$$E(x_{a1})\ddot{x}_{a1} + F(x_{a1})\dot{x}_{a1}^2 = \sum_{i=0}^{\infty} a_{2i+1}\cos\left[(2i+1)\tau\right] \tag{18}$$

$$G(x_{a1}) = \sum_{i=0}^{\infty} b_{2i+1}\cos\left[(2i+1)\tau\right] \tag{19}$$

$$E(x_{a1}) = \sum_{i=0}^{\infty} c_{2i} \cos(2i\tau) \tag{20}$$

$$F(x_{a1})\dot{x}_{a1} = \sum_{i=0}^{\infty} d_{2(i+1)} \sin\left[2(i+1)\tau\right] \tag{21}$$

$$E_x(x_{a1})\ddot{x}_{a1} + F_x(x_{a1})\dot{x}_{a1}^2 = \sum_{i=0}^{\infty} e_{2i} \cos(2i\tau) \tag{22}$$

$$G_x(x_{a1}) = \sum_{i=0}^{\infty} f_{2i} \cos(2i\tau) \tag{23}$$

where a_i, b_i, c_i, d_i, e_i and f_i are Fourier series coefficients that can be determined by

$$a_{2i+1} = \frac{4}{\pi}\int_0^{\pi/2}\left[E(x_{a1})\ddot{x}_{a1} + F(x_{a1})\dot{x}_{a1}^2\right]\cos\left[(2i+1)\tau\right]d\tau, \quad i = 0,1,2.... \tag{24}$$

$$b_{2i+1} = \frac{4}{\pi}\int_0^{\pi/2} G(x_{a1})\cos\left[(2i+1)\tau\right]d\tau, \quad i = 0,1,2.... \tag{25}$$

$$c_{2i} = \frac{4}{\pi}\int_0^{\pi/2} E(x_{a1})\cos(2i\tau)d\tau, \quad i = 0,1,2.... \tag{26}$$

$$d_{2(i+1)} = \frac{8}{\pi}\int_0^{\pi/2} F(x_{a1})\dot{x}_{a1}\sin\left[2(i+1)\tau\right]d\tau, \quad i = 0,1,2.... \tag{27}$$

$$e_{2i} = \frac{4}{\pi}\int_0^{\pi/2}\left[E_x(x_{a1})\ddot{x}_{a1} + F_x(x_{a1})\dot{x}_{a1}^2\right]\cos(2i\tau)d\tau, \quad i = 0,1,2.... \tag{28}$$

$$f_{2i} = \frac{4}{\pi}\int_0^{\pi/2} G_x(x_{a1})\cos(2i\tau)d\tau, \quad i = 0,1,2.... \tag{29}$$

For the first-order analytical approximation, we set

$$\Delta x_{a1}(\tau) = 0, \qquad \Delta\Omega_{a1} = 0 \tag{30}$$

and

$$x_{a1}(\tau) = A\cos\tau \tag{31}$$

The above equation satisfies the initial conditions given in Eq. (13). Substituting Eqs. (18)–(23), (30) and (31) into Eq. (17), expanding the resulting expression into a trigonometric series and setting the coefficient of $\cos\tau$ to zero, we obtain

$$\Omega_{a1}\left(A\right) = -\frac{b_1}{a_1} \tag{32}$$

Hence, the first-order approximate periodic solution $x_{a1}(t)$ is

$$x_{a1}(t) = A\cos\tau, \qquad \tau = \sqrt{\Omega_{a1}\left(A\right)}t \tag{33}$$

For the second-order analytical approximation, we set

$$\Delta x_{a1}(\tau) = z_1(\cos\tau - \cos 3\tau) \tag{34}$$

Inserting Eqs. (18)–(23), (31) and (34) into Eq. (17), expanding the resulting expression in a trigonometric series and setting the coefficients of $\cos\tau$ and $\cos 3\tau$ to zero, we obtain

$$z_1(A) = -\frac{2C_1}{A_2 + B_2\Omega_{a1}} \tag{35}$$

$$\Delta\Omega_{a1}(A) = -\frac{2C_1(B_1 + A_1\Omega_{a1})}{a_1(B_2 + A_2\Omega_{a1})} \tag{36}$$

where

$$A_1 = \frac{1}{2}\left(-c_0 + 8c_2 + 9c_4 + 2d_2 + 3d_4 + e_0 - e_4\right) \tag{37}$$

$$B_1 = \frac{1}{2}\left(f_0 - f_4\right) \tag{38}$$

$$A_2 = -a_1 f_0 - a_3 f_0 + a_1 f_2 + a_1 f_4 + a_3 f_4 - a_1 f_6 \tag{39}$$

$$\begin{aligned} B_2 = 9a_1c_0 + a_3c_0 - a_1c_2 - 8a_3c_2 - a_1c_4 - 9a_3c_4 + 9a_1c_6 + a_1d_2 - 2a_3d_2 - \\ a_1d_4 - 3a_3d_4 + 3a_1d_6 - a_1e_0 - a_3e_0 + a_1e_2 + a_1e_4 + a_3e_4 - a_1e_6 \end{aligned} \tag{40}$$

$$C_1 = a_3 b_1 - a_1 b_3 \tag{41}$$

Therefore, the second-order approximate periodic solution $x_{a2}(t)$ is

$$x_{a2}(t) = x_{a1}(\tau) + \Delta x_{a1}(\tau) = (A + z_1)\cos\tau - z_1\cos 3\tau, \quad \tau = \sqrt{\Omega_{a2}(A)}\,t \tag{42}$$

where

$$\Omega_{a2}(A) = \Omega_{a1}(A) + \Delta\Omega_{a1}(A) = -\frac{b_1}{a_1} - \frac{2C_1\left[B_1 + A_1(-b_1/a_1)\right]}{a_1\left[B_2 + A_2(-b_1/a_1)\right]} \tag{43}$$

Based on the above equations, the analytical approximate solutions for the symmetric oscillation of the nonlinear system (1) around the stable equilibrium point x_1 can be derived.

3.2 Analytical approximations for asymmetric oscillations

In addition, there exist heteroclinic orbits [29, 30] where the nonlinear system (1) has more than one equilibrium points. Under this condition, the system can also oscillate around other stable equilibrium points with an asymmetric limit $[A', A]$ where A' and A have the same energy level in accordance with the principle of conservation of energy [31]

$$V(A) = V(A') \tag{44}$$

in which A' can be expressed as a function of A.

When the system oscillates asymmetrically, a new variable is introduced as follows:

$$u = x - \lambda \tag{45}$$

Eq. (1) can be derived as

$$\tilde{E}(u)\frac{d^2u}{dt^2} + \tilde{F}(u)\left(\frac{du}{dt}\right)^2 + \tilde{G}(u) = 0 \tag{46}$$

with the following initial conditions

$$u(0) = B = A - \lambda\,, \quad \frac{du(0)}{dt} = 0 \tag{47}$$

in which

$$\tilde{E}(u) = 1 + \alpha_1\lambda^2 + 2\alpha_1\lambda u + \alpha_1 u^2 \tag{48}$$

$$\tilde{F}(u) = \alpha_1\lambda + \alpha_1 u \tag{49}$$

$$\tilde{G}(u) = \gamma_1 u + \gamma_2 u^2 + \gamma_3 u^3 + \gamma_4 u^4 + \gamma_5 u^5 \tag{50}$$

where $\gamma_1 = \alpha_2 + 3\alpha_3\lambda^2 + 5\alpha_4\lambda^4$, $\gamma_2 = 3\alpha_2\lambda + 10\alpha_4\lambda^3$, $\gamma_3 = \alpha_3 + 10\alpha_4\lambda^2$, $\gamma_4 = 5\alpha_4\lambda$ and $\gamma_5 = \alpha_4$. Note that λ is the coordinate value of the corresponding equilibrium point.

In Eq. (46), the system oscillates within an asymmetric bound $\left[B', B\right]$ $\left(B' = A' - \lambda\right)$ around the stable equilibrium point $u = 0$. It is noted that $\tilde{E}(-u) \neq -\tilde{E}(u)$, $\tilde{F}(-u) \neq -\tilde{F}(u)$, $\tilde{G}(-u) \neq -\tilde{G}(u)$. To solve such a mixed-parity nonlinear system, two newly odd nonlinear systems are introduced [31] as follows:

$$H(u)\frac{d^2u}{dt^2} + I(u)\left(\frac{du}{dt}\right)^2 + J(u) = 0\,,\ u(0) = B\,,\ \frac{du(0)}{dt} = 0 \tag{51}$$

and

$$K(u)\frac{d^2u}{dt^2} + L(u)\left(\frac{du}{dt}\right)^2 + M(u) = 0\,,\ u(0) = -B'(B' < 0)\,,\ \frac{du(0)}{dt} = 0 \tag{52}$$

where

$$H(u) = \begin{cases} \tilde{E}(u), & u \geq 0 \\ \tilde{E}(-u), & u < 0 \end{cases},\quad I\left(u\right) = \begin{cases} \tilde{F}(u), & u \geq 0 \\ -\tilde{F}(-u), & u < 0 \end{cases},\quad J(u) = \begin{cases} \tilde{G}(u), & u \geq 0 \\ -\tilde{G}(-u), & u < 0 \end{cases} \tag{53}$$

and

$$K(u) = \begin{cases} \tilde{E}(-u), & u > 0 \\ \tilde{E}(u), & u \leq 0 \end{cases},\quad L(u) = \begin{cases} -\tilde{F}(-u), & u > 0 \\ \tilde{F}(u), & u \leq 0 \end{cases},\quad M(u) = \begin{cases} -\tilde{G}(-u), & u > 0 \\ \tilde{G}(u), & u \leq 0 \end{cases} \tag{54}$$

Equations (51) and (52) can be solved independently by the NHB method as mentioned in Section 3.1. To consider the asymmetric oscillation of the system (1), the analytical approximations are mathematically formulated by combining the piecewise approximate solutions obtained from Eqs. (51) and (52).

According to Eqs. (51) and (52), the first-order approximate periodic solution ($x_{a1}(t)$) for the asymmetric oscillation of the nonlinear system (1) is

$$x_{a1}(t)=\begin{cases} u_{11}(t)+\lambda, & 0\le t\le \dfrac{T_{11}(B)}{4} \\ u_{12}\left(t-\dfrac{T_{11}(B)}{4}+\dfrac{T_{12}(B')}{4}\right)+\lambda, & \dfrac{T_{11}(B)}{4}\le t\le \dfrac{T_{11}(B)}{4}+\dfrac{T_{12}(B')}{2} \\ u_{11}\left(t+\dfrac{T_{11}(B)}{2}-\dfrac{T_{12}(B')}{2}\right)+\lambda, & \dfrac{T_{11}(B)}{4}+\dfrac{T_{12}(B')}{2}\le t\le \dfrac{T_{11}(B)+T_{12}(B')}{2} \end{cases} \tag{55}$$

and the first-order approximate period (T_{a1}) and frequency ($\sqrt{\Omega_{a1}}$) are

$$T_{a1}(A)=\frac{T_{11}(B)+T_{12}(B')}{2} \quad \text{and} \quad \sqrt{\Omega_{a1}(A)}=\frac{2\pi}{T_{a1}(A)} \tag{56}$$

where the subscripts "11" and "12" of T and u denote the first-order approximate periods and the corresponding periodic solutions for the systems (51) and (52), respectively.

Besides, the second-order approximate periodic solution ($x_{a2}(t)$) for the asymmetric oscillation of the nonlinear system (1) is

$$x_{a2}(t)=\begin{cases} u_{21}(t)+\lambda, & 0\le t\le \dfrac{T_{21}(B)}{4} \\ u_{22}\left(t-\dfrac{T_{21}(B)}{4}+\dfrac{T_{22}(B')}{4}\right)+\lambda, & \dfrac{T_{21}(B)}{4}\le t\le \dfrac{T_{21}(B)}{4}+\dfrac{T_{22}(B')}{2} \\ u_{21}\left(t+\dfrac{T_{21}(B)}{2}-\dfrac{T_{22}(B')}{2}\right)+\lambda, & \dfrac{T_{21}(B)}{4}+\dfrac{T_{22}(B')}{2}\le t\le \dfrac{T_{21}(B)+T_{22}(B')}{2} \end{cases} \tag{57}$$

and the second-order approximate period (T_{a2}) and frequency ($\sqrt{\Omega_{a2}}$) are

$$T_{a2}(A)=\frac{T_{21}(B)+T_{22}(B')}{2} \quad \text{and} \quad \sqrt{\Omega_{a2}(A)}=\frac{2\pi}{T_{a2}(A)} \tag{58}$$

where the subscripts "21" and "22" of T and u denote the second-order approximate periods and the corresponding periodic solutions for the systems (51) and (52), respectively.

4. Results and discussion

In this section, the approximate solutions for various parameters α_1, α_2, α_3 and α_4 are presented to verify the accuracy of NHB method with respect to the Runge-Kutta method and other methods, e.g., homotopy perturbation method (HPM) [7, 32]. For a symmetric oscillation, the exact frequency of the nonlinear problem (1) in terms of an implicit form is given by

$$\omega_e(A) = \pi / \int_0^{\frac{\pi}{2}} \sqrt{\frac{1+\alpha_1 (A\cos\theta)^2}{2\left[V(A) - V(A\cos\theta)\right]}} (-A\cos\theta) d\theta \tag{59}$$

where $V(\square)$ is the potential energy of the system (1).

For an asymmetric oscillation, the exact frequency of the nonlinear system (1) can be constructed by

$$\omega_e(A) = \frac{2\omega_{e1}(B)\omega_{e2}(B')}{\omega_{e1}(B) + \omega_{e2}(B')} \tag{60}$$

where $\omega_{e1}(B)$ and $\omega_{e2}(B')$ are the exact frequencies of the corresponding systems (51) and (52), respectively.

Consider cases 1 and 3, the first-order and second-order approximate frequencies (i.e., $\sqrt{\Omega_{a1}}$ and $\sqrt{\Omega_{a2}}$) of the NHB method are compared with the exact solution (ω_e) and the HPM solution (ω_{HPM}) in Tables 2-5. The first-order approximate frequencies derived from the NHB method are the same as those results of the HPM [7]. They have good agreement with the corresponding exact solutions when the initial amplitude is small. When the initial amplitude A larger than 5, these two analytical approximations are not acceptable. However, the second-order approximate frequencies have good agreement with the exact results for small as well as large initial amplitudes. Figures 6 and 7 show the results of the first-order and second-order approximate periodic solutions (i.e., $x_{a1}(t)$ and $x_{a2}(t)$) obtained from the NHB method and the corresponding numerical solution ($x_e(t)$) obtained from the Runge-Kutta method. We clearly observe that the accuracy of the second-order approximate periodic solution is higher than the first-order approximate periodic solution.

On the other hand, the results of other two examples for case 5 are given in Tables 6 and 7 for the asymmetric and symmetric oscillations around three stable equilibrium points, respectively. Both the first-order and second-order approximate frequencies are highly consistent with the exact solution due to a small initial deviation to the corresponding equilibrium points. The time history responses of the analytical approximate periodic solutions (i.e., $x_{a1}(t)$ and $x_{a2}(t)$) and numerical solution ($x_e(t)$) are depicted in Figs. 8−10. The absolute errors in Figs. 8−10 show that the accuracy of the second-order approximate periodic solution is still better than the first-order approximate periodic solution when comparing with the numerical one.

5. Conclusions

This paper presents a qualitative and quantitative study to investigate a triple-well non-natural system that is governed by a quadratic velocity term and an odd-parity nonlinearity. The effect of a negative linear stiffness on the nonlinear system is also studied. In terms of qualitative analysis, the equilibrium points and its trajectories among the influence of various governing parameters are presented in detail. The possible motions of the nonlinear system according to the initial amplitudes and the governing parameters are provided. Based on the analysis, it is found that there exist three different types of equilibrium points, i.e., center, saddle point and degenerate singular point. There exist heteroclinic and homoclinic orbits under different equilibrium states. For quantitative analysis, the NHB method is applied to construct accurate lower-order analytical approximations. The analytical approximation results are in good agreement with the exact solution, it is also valid for large amplitudes of oscillation and governing parameters. Both symmetric and asymmetric oscillations around different equilibrium points are also investigated. The present work provides a better understanding of the nonlinear non-natural system for engineering design and control.

Acknowledgements

The work described in this paper was supported by the National Natural Science Foundation of China (Grant Nos. 11602210 and 11672259) and the Early Career Scheme from the Research Grants Council of the Hong Kong Special Administrative Region (Project No. PolyU 252026/16E).

References

[1] Pandey, A., Ghose-Choudhury, A., and Guha, P., 2017, “Chiellini integrability and quadratically damped oscillators,” Int J Non-Linear Mech, 92, pp.153−159.

[2] Meirovitch, L., Methods of analytical dynamics. New York: McGraw-Hill; 1970.

[3] Nayfeh, A.H., and Mook, D.T., Nonlinear oscillations. Wiley; 1995.

[4] Lai, S.K., and Chow, K.W., 2012, “Exact solutions for oscillators with quadratic damping and mixed-parity nonlinearity,” Phys Scr, 85, 045006.

[5] Bayat, M., Pakar, I., and Bayat, M., 2013, “Analytical solution for nonlinear vibration of an eccentrically reinforced cylindrical shell,” Steel Compos Struct, 14, pp. 511−521.

[6] Bayat, M., Pakar, I., and Cveticanin, L., 2014, “Nonlinear vibration of stringer shell by means of extended Hamiltonian approach,” Arch Appl Mech, 84, pp. 43−50.

[7] Pakar, I., and Bayat, M., 2015, “Nonlinear vibration of stringer shell: An analytical approach,” Proc Inst Mech Eng Part E-J Process Mech Eng, 229, pp. 44−51.

[8] Rao, G.V., 2003, “Large amplitude vibrations of slender uniform beams on elastic foundation,” Indian J Eng Mat Sci, 10, pp. 87−91.

[9] Hui, C.K., Lee, Y.Y., and Reddy, J.N., 2011, “Approximate elliptical integral solution for the large amplitude free vibration of a rectangular single mode plate backed by a multi-acoustic mode cavity,” Thin-Walled Struct, 49, pp. 1191−1194.

[10] Tang, Y., and Yang, T., 2018, “Post-buckling behaviour and nonlinear vibration analysis of a fluid-conveying pipe composed of functionally grade material,” Compos Struct, 185, pp. 393−400.

[11] Sun, Y., Yu, Y., and Liu, B., 2015, “Closed form solutions for predicting static and dynamic buckling behaviours of a drillstring in a horizontal well,” Eur J Mech A-Solids 49, pp. 362−372.

[12] Daqaq, M.F., Masana, R., Erturk, A., and Quinn, D.D., 2014, “On the role of nonlinearities in vibratory energy harvesting: A critical review and discussion,” Appl Mech Rev, 66, 040801.

[13] Vakakis, A.F., Gendelman, O.V., Bergman, L.A., McFarland, D.M., Kerschen, G., and Lee, Y.S., Nonlinear targeted energy transfer in mechanical and structural systems I & II. Springer: 2009.

[14] Harne, R.L., and Wang, K.W., 2013, “A review of the recent research on vibration energy harvesting via bistable systems,” Smart Mater Struct, 22, 023001.

[15] Lenci, S., Menditto, G., and Tarantino, A.M., 1999, "Homoclinic and heteroclinic bifurcations in the nonlinear dynamics of a beam resting on an elastic substrate," Int J Non-Linear Mech, 34, pp. 615−632.

[16] Hamdan, M.N., and Shabaneh, N.H., 1997, "On the large amplitude free vibrations of a restrained uniform beam carrying an intermediate lumped mass," J Sound Vibr, 199, pp. 711−736.

[17] Lai, S.K., Lim, C.W., Lin, Z., and Zhang, W., 2011, "Analytical analysis for large-amplitude oscillation of a rotational pendulum system," Appl Math Comput, 217, pp. 6115−6124.

[18] Hamdan, M.N., and Dado, M.H., 1997, "Large amplitude free vibrations of a uniform cantilever beam carrying an intermediate lumped mass and rotary inertia," J Sound Vibr 206, pp. 151−168.

[19] Jarrar, F.S.M. and Hamdan, M.N., 2007, "Nonlinear vibrations and buckling of a flexible rotating beam: A prescribed torque approach," Mech Mach Theory, 42, pp. 919−939.

[20] Guo, Z., and Zhang, W., 2016, "The spreading residue harmonic balance study on the vibration frequencies of tapered beams," Appl Math Model, 40, pp. 7195−7203.

[21] Wu, B.S., Lim, C.W., and He, L.H., 2003, "A new method for approximate analytical solutions to nonlinear oscillations of nonnatural systems," Nonlinear Dyn. 32, pp. 1−13.

[22] Mohanasubha, R., and Senthilvelan, M., 2017, "On the symmetries of a non-polynomial oscillator," Commun Nonlinear Sci Numer Simul, 43, pp. 111−117.

[23] Wu, B.S., Sun, W.P., and Lim, C.W., 2006, "An analytical approximate technique for a class of strongly non-linear oscillators," Int J Non-Linear Mech, 41, pp. 766−774.

[24] Wu, B.S., Liu, W.J., Chen, X., and Lim, C.W., 2017, "Asymptotic analysis and accurate approximate solutions for strongly nonlinear conservative symmetric oscillators," Appl Math Model, 49, pp. 243−254.

[25] Sun, W.P., and Wu, B.S., 2008, "Accurate analytical approximate solutions to general strong nonlinear oscillators," Nonlinear Dyn, 51, pp. 277−287.

[26] Lai, S.K., Lim, C.W., Xiang, Y., and Zhang, W., 2009, "On asymptotic analysis for large amplitude nonlinear free vibration of simply supported laminated plates," J Vib Acoust-Trans. ASME, 131, 051010.

[27] Yu, Y., Sun, Y., and Zang, L., 2013, "Analytical solution for initial postbuckling deformation of the sandwich beams including transverse shear," J. Eng. Mech. 139, pp. 1084−1090.

[28] Liu, W., Wu, B., and Lim, C.W., 2017, Linear and nonlinear free vibrations of electrostatically actuated micro-/nanomechanical resonators. Microsyst Technol, 23, pp. 113−123.

[29] Yao, M.H., Zhang, W., 2007, "Shilnikov-type multipulse orbits and chaotic dynamics of a parametrically and externally excited rectangular thin plate," Int J Bifurcation Chaos 17, pp. 851−875.

[30] Algaba, A., Fernandez-Sanchez, F., Merino, M., 2013, "On Shilnikov analysis of homoclinic and heteroclinic orbits of the T-system," J Comput. Nonlinear Dyn. 8, 027001.

[31] Wu, B.S., and Lim, C.W., 2004, "Large amplitude nonlinear oscillations of a general conservative system," Int J Non-Linear Mech 39, pp. 859−870.

[32] Neamaty, A., Agheli, B., and Darzi, R., 2015, "Numerical solution of high-order fractional Volterra integro-differential equations by variational homotopy perturbation iteration method," J Comput. Nonlinear Dyn. 10, 061023.

Captions of Tables

Table 1 **Equilibrium states of the nonlinear system (1).**

Table 2 **Comparison of approximate and exact frequencies for** $\alpha_1 = 0.5$**,** $\alpha_2 = 2$**,** $\alpha_3 = 2$ **and** $\alpha_4 = 1.3$**.**

Table 3 **Comparison of approximate and exact frequencies for** $\alpha_1 = 0.5$ **,** $\alpha_2 = 2$ **,** $\alpha_3 = -0.2$ **and** $\alpha_4 = 1.3$**.**

Table 4 **Comparison of approximate and exact frequencies for** $\alpha_1 = 0.1$ **,** $\alpha_2 = 1$ **,** $\alpha_3 = 0.5$ **and** $\alpha_4 = 0.27$**.**

Table 5 **Comparison of approximate and exact frequencies for** $\alpha_1 = 0.1$ **,** $\alpha_2 = 1$ **,** $\alpha_3 = -0.5$ **and** $\alpha_4 = 0.27$**.**

Table 6 **Comparison of approximate and exact frequencies for** $\alpha_1 = 0.5$ **,** $\alpha_2 = 2$ **,** $\alpha_3 = -5.7$ **and** $\alpha_4 = 1.3$**.**

Table 7 **Comparison of approximate and exact frequencies for** $\alpha_1 = 0.1$ **,** $\alpha_2 = 1$ **,** $\alpha_3 = -1.5$ **and** $\alpha_4 = 0.27$**.**

Captions of Figures

Fig. 1. **Phase planes for the nonlinear system with one equilibrium point.**

Fig. 2. **Phase planes for the nonlinear system with three equilibrium points.**

Fig. 3. **Phase planes for the nonlinear system with five equilibrium points.**

Fig. 4. **Bifurcation behaviour of the nonlinear system affected by the parameters** α_2 **and** α_3**.**

Fig. 5. **Bifurcation behaviour of the nonlinear system affected by the parameters** α_1 **and** α_3**.**

Fig. 6. **Comparison of analytical approximate periodic solutions with numerical solution for** $\alpha_1 = 0.5$**,** $\alpha_2 = 2$**,** $\alpha_3 = -0.2$**,** $\alpha_4 = 1.3$ **and** $A = 10$**.**

Fig. 7. **Comparison of analytical approximate periodic solutions with numerical solution for** $\alpha_1 = 0.1$**,** $\alpha_2 = 1$**,** $\alpha_3 = -0.5$**,** $\alpha_4 = 0.27$ **and** $A = 100$**.**

Fig. 8. **(a) Comparison of analytical approximate periodic solutions with numerical solution for** $\alpha_1 = 0.1$**,** $\alpha_2 = 1$**,** $\alpha_3 = -1.5$**,** $\alpha_4 = 0.27$ **and** $A = 0.1$**; (b) Comparison of the absolute errors between the approximate and numerical solutions.**

Fig. 9. **(a) Comparison of analytical approximate periodic solutions with numerical solution for** $\alpha_1 = 0.1$ **,** $\alpha_2 = 1$ **,** $\alpha_3 = -1.5$ **,** $\alpha_4 = 0.27$ **and** $A = 2.2865$ **; (b) Comparison of the absolute errors between the approximate and numerical solutions.**

Fig. 10. (a) Comparison of analytical approximate periodic solutions with numerical solution for $\alpha_1 = 0.1$, $\alpha_2 = 1$, $\alpha_3 = -1.5$, $\alpha_4 = 0.27$ and $A = -2.0865$; (b) Comparison of the absolute errors between the approximate and numerical solutions.

Table 1 Equilibrium states of the nonlinear system (1).

<table>
<tr><th>Case number</th><th colspan="2">Governing parameters</th><th>Number of equilibrium points</th><th>Equilibrium points and orbital characteristics around centers</th></tr>
<tr><td>1</td><td colspan="2">$\alpha_1 > 0$, $\alpha_2 > 0$, $\alpha_3 > 0$, $\alpha_4 > 0$</td><td>1</td><td>$x_1 = 0$ (center, symmetric orbit)</td></tr>
<tr><td>2</td><td colspan="2">$\alpha_1 > 0$, $\alpha_2 < 0$, $\alpha_3 > 0$, $\alpha_4 > 0$</td><td>3</td><td>$x_1 = 0$ (saddle point)
$x_{2,3} = \pm R3$ (center, asymmetric orbit)</td></tr>
<tr><td>3</td><td rowspan="3">$\alpha_1 > 0$,
$\alpha_2 > 0$,
$\alpha_3 < 0$,
$\alpha_4 > 0$</td><td>$\alpha_3^2 - 4\alpha_2\alpha_4 < 0$</td><td>1</td><td>$x_1 = 0$ (center, symmetric orbit)</td></tr>
<tr><td>4</td><td>$\alpha_3^2 - 4\alpha_2\alpha_4 = 0$</td><td>3</td><td>$x_1 = 0$ (center, symmetric orbit)
$x_{2,3} = \pm R1$ (degenerate singular point)</td></tr>
<tr><td>5</td><td>$\alpha_3^2 - 4\alpha_2\alpha_4 > 0$</td><td>5</td><td>$x_1 = 0$ (center, symmetric orbit)
$x_{2,3} = \pm R2$ (saddle point)
$x_{4,5} = \pm R3$ (center, asymmetric orbit)</td></tr>
<tr><td>6</td><td colspan="2">$\alpha_1 > 0$, $\alpha_2 > 0$, $\alpha_3 > 0$, $\alpha_4 < 0$</td><td>3</td><td>$x_1 = 0$ (center, symmetric orbit)
$x_{2,3} = \pm R2$ (saddle point)</td></tr>
<tr><td>7</td><td colspan="2">$\alpha_1 > 0$, $\alpha_2 < 0$, $\alpha_3 < 0$, $\alpha_4 > 0$</td><td>3</td><td>$x_1 = 0$ (saddle point)
$x_{2,3} = \pm R3$ (center, asymmetric orbit)</td></tr>
<tr><td>8</td><td rowspan="3">$\alpha_1 > 0$,
$\alpha_2 < 0$,
$\alpha_3 > 0$,
$\alpha_4 < 0$</td><td>$\alpha_3^2 - 4\alpha_2\alpha_4 < 0$</td><td>1</td><td>$x_1 = 0$ (saddle point)</td></tr>
<tr><td>9</td><td>$\alpha_3^2 - 4\alpha_2\alpha_4 = 0$</td><td>3</td><td>$x_1 = 0$ (saddle point)
$x_{2,3} = \pm R1$ (degenerate singular point)</td></tr>
<tr><td>10</td><td>$\alpha_3^2 - 4\alpha_2\alpha_4 > 0$</td><td>5</td><td>$x_1 = 0$ (saddle point)
$x_{2,3} = \pm R3$ (center, asymmetric orbit)
$x_{4,5} = \pm R2$ (saddle point)</td></tr>
<tr><td>11</td><td colspan="2">$\alpha_1 > 0$, $\alpha_2 > 0$, $\alpha_3 < 0$, $\alpha_4 < 0$</td><td>3</td><td>$x_1 = 0$ (center, symmetric orbit)
$x_{2,3} = \pm R2$ (saddle point)</td></tr>
</table>

Note: $R1 = \sqrt{\frac{-\alpha_3}{2\alpha_4}}$, $R2 = \sqrt{\frac{-\alpha_3 - \sqrt{\alpha_3^2 - 4\alpha_2\alpha_4}}{2\alpha_4}}$ and $R3 = \sqrt{\frac{-\alpha_3 + \sqrt{\alpha_3^2 - 4\alpha_2\alpha_4}}{2\alpha_4}}$.

Table 2 Comparison of approximate and exact frequencies for $\alpha_1 = 0.5$, $\alpha_2 = 2$, $\alpha_3 = 2$ and $\alpha_4 = 1.3$.

A	ω_{HPM} [7]	$\sqrt{\Omega_{a1}}$, Eq. (32)	$\sqrt{\Omega_{a2}}$, Eq. (43)	ω_e, Eq. (59)
0.2	1.42860	1.42860	1.42860	1.42860
0.5	1.51099	1.51099	1.51091	1.51090
1.2	2.07308	2.07308	2.07268	2.07151
2	3.24037	3.24037	3.28111	3.27386
5	8.68858	8.68858	9.45407	9.39663
10	17.8432	17.8432	20.1124	20.0870
20	35.9595	35.9595	41.0192	41.2150
100	180.258	180.258	206.475	208.430

Table 3 Comparison of approximate and exact frequencies for $\alpha_1 = 0.5$, $\alpha_2 = 2$, $\alpha_3 = -0.2$ and $\alpha_4 = 1.3$.

A	ω_{HPM} [7]	$\sqrt{\Omega_{a1}}$, Eq. (32)	$\sqrt{\Omega_{a2}}$, Eq. (43)	ω_e, Eq. (59)
0.2	1.40554	1.40554	1.40555	1.40555
0.5	1.37654	1.37654	1.37689	1.37689
1.2	1.59706	1.59706	1.60129	1.59977
2	2.68328	2.68328	2.70640	2.69843
5	8.35474	8.35474	9.07751	9.02539
10	17.6635	17.6635	19.9041	19.8821
20	35.8686	35.8686	40.9120	41.1093
100	180.240	180.240	206.454	208.409

Table 4 Comparison of approximate and exact frequencies for $\alpha_1 = 0.1$, $\alpha_2 = 1$, $\alpha_3 = 0.5$ and $\alpha_4 = 0.27$.

A	ω_{HPM} [7]	$\sqrt{\Omega_{a1}}$, Eq. (32)	$\sqrt{\Omega_{a2}}$, Eq. (43)	ω_e, Eq. (59)
0.2	1.00660	1.00660	1.00660	1.00660
0.5	1.04435	1.04435	1.04420	1.04419
1.2	1.32777	1.32777	1.32138	1.32091
2	2.08167	2.08167	2.04997	2.04623
5	7.17538	7.17538	7.25945	7.23658
10	16.9607	16.9607	18.2688	18.1618
20	35.9570	35.9570	40.3727	40.2831
100	183.549	183.549	210.094	211.840

Table 5 Comparison of approximate and exact frequencies for $\alpha_1 = 0.1$, $\alpha_2 = 1$, $\alpha_3 = -0.5$ and $\alpha_4 = 0.27$.

A	ω_{HPM} [7]	$\sqrt{\Omega_{a1}}$, Eq. (32)	$\sqrt{\Omega_{a2}}$, Eq. (43)	ω_e, Eq. (59)
0.2	0.99162	0.99162	0.99161	0.99161
0.5	0.95157	0.95157	0.95139	0.95140
1.2	0.86921	0.86921	0.86940	0.86936
2	1.35401	1.35401	1.32931	1.32155
5	6.56908	6.56908	6.61769	6.59292
10	16.5881	16.5881	17.8510	17.7492
20	35.7578	35.7578	40.1412	40.0554
100	183.508	183.508	210.046	211.792

Table 6 Comparison of approximate and exact frequencies for $\alpha_1 = 0.5$, $\alpha_2 = 2$, $\alpha_3 = -5.7$ and $\alpha_4 = 1.3$.

A	Equilibrium point at	$\sqrt{\Omega_{a1}}$, Eq. (32)	$\sqrt{\Omega_{a2}}$, Eq. (43)	ω_e , Eq. (59)
0.1	x_1=0	1.39730	1.39728	1.39728

A	Equilibrium point at	$\sqrt{\Omega_{a1}}$, Eq. (56)	$\sqrt{\Omega_{a2}}$, Eq. (58)	ω_e , Eq. (60)
2.1	x_4=2	3.51270	3.51244	3.51264
−1.9	x_5=−2	3.51882	3.51862	3.51877

Note: The system oscillates symmetrically around x_1, but asymmetrically around x_4 or x_5.

Table 7 Comparison of approximate and exact frequencies for $\alpha_1 = 0.1$, $\alpha_2 = 1$, $\alpha_3 = -1.5$ and $\alpha_4 = 0.27$.

A	Equilibrium point at	$\sqrt{\Omega_{a1}}$, Eq. (32)	$\sqrt{\Omega_{a2}}$, Eq. (43)	ω_e , Eq. (59)
0.1	x_1=0	0.99412	0.99412	0.99412

A	Equilibrium point at	$\sqrt{\Omega_{a1}}$, Eq. (56)	$\sqrt{\Omega_{a2}}$, Eq. (58)	ω_e , Eq. (60)
2.2865	x_4=2.1865	2.62193	2.62042	2.62161
−2.0865	x_5=−2.1865	2.62691	2.62562	2.62665

Note: The system oscillates symmetrically around x_1, but asymmetrically around x_4 or x_5.

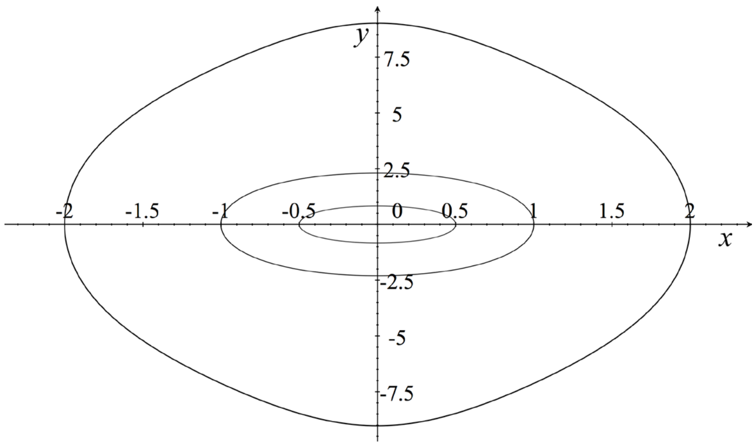

(a) Case 1 and Case 3

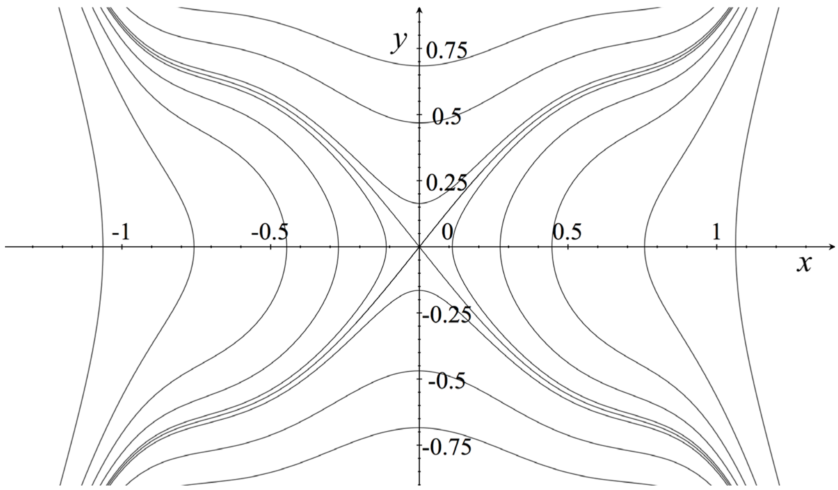

(b) Case 8

Fig. 1. Phase planes for the nonlinear system with one equilibrium point.

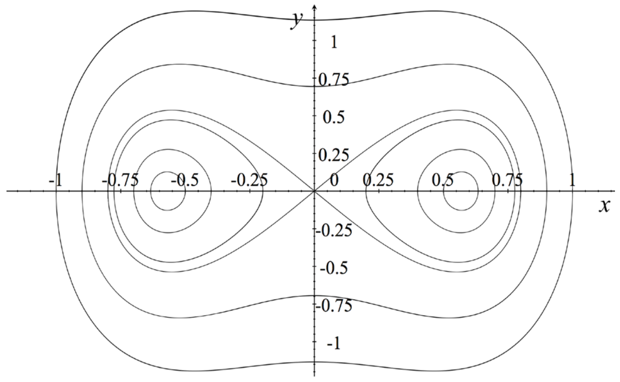

(a) Case 2 and Case 7

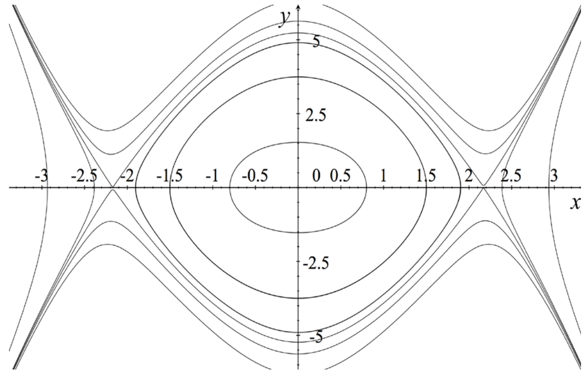

(b) Case 6 and Case 11

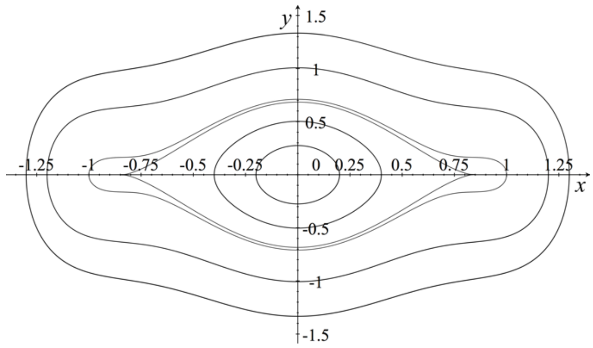

(c) Case 4

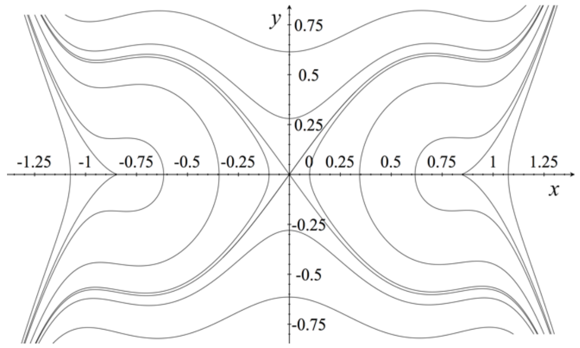

(d) Case 9

Fig. 2. Phase planes for the nonlinear system with three equilibrium points.

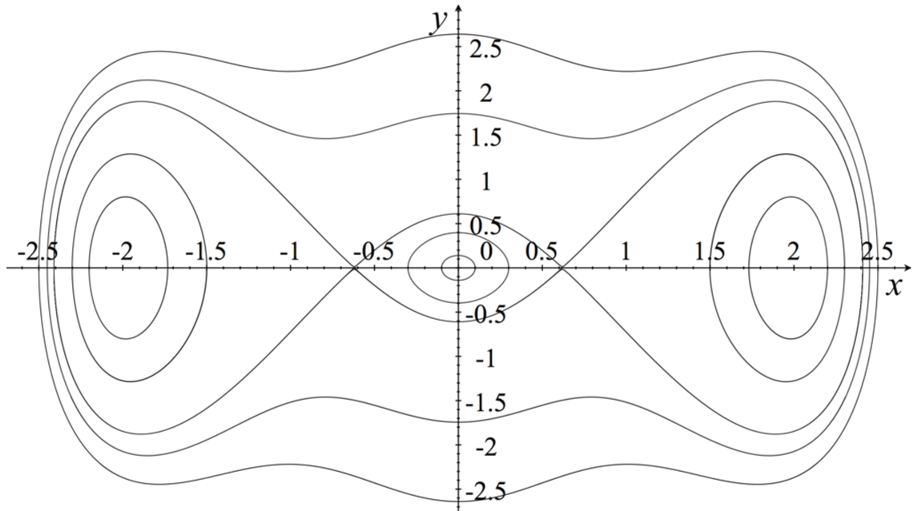

(a) Case 5

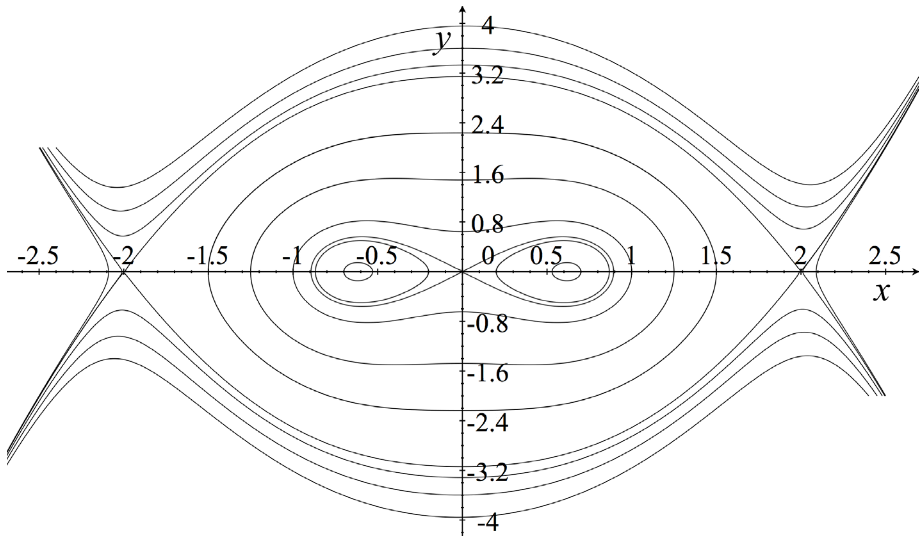

(b) Case 10

Fig. 3. Phase planes for the nonlinear system with five equilibrium points.

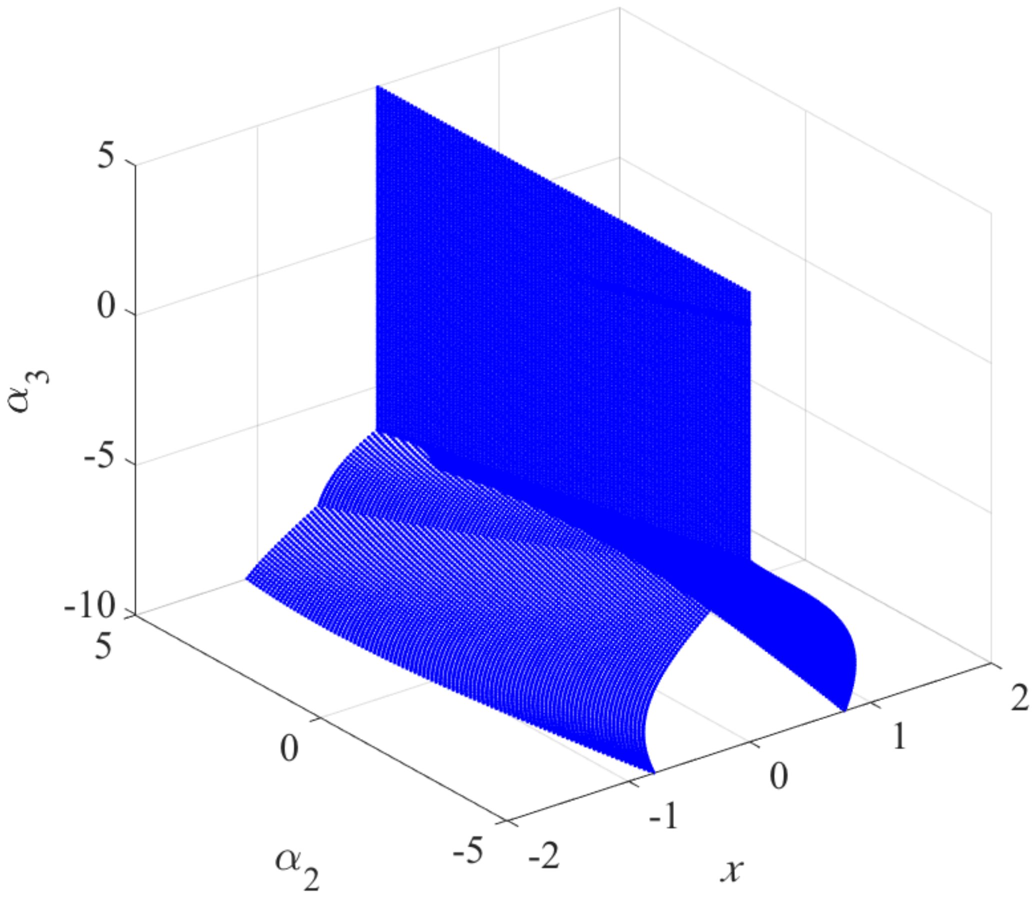

Fig. 4. Bifurcation behaviour of the nonlinear system affected by the parameters α_2 and α_3.

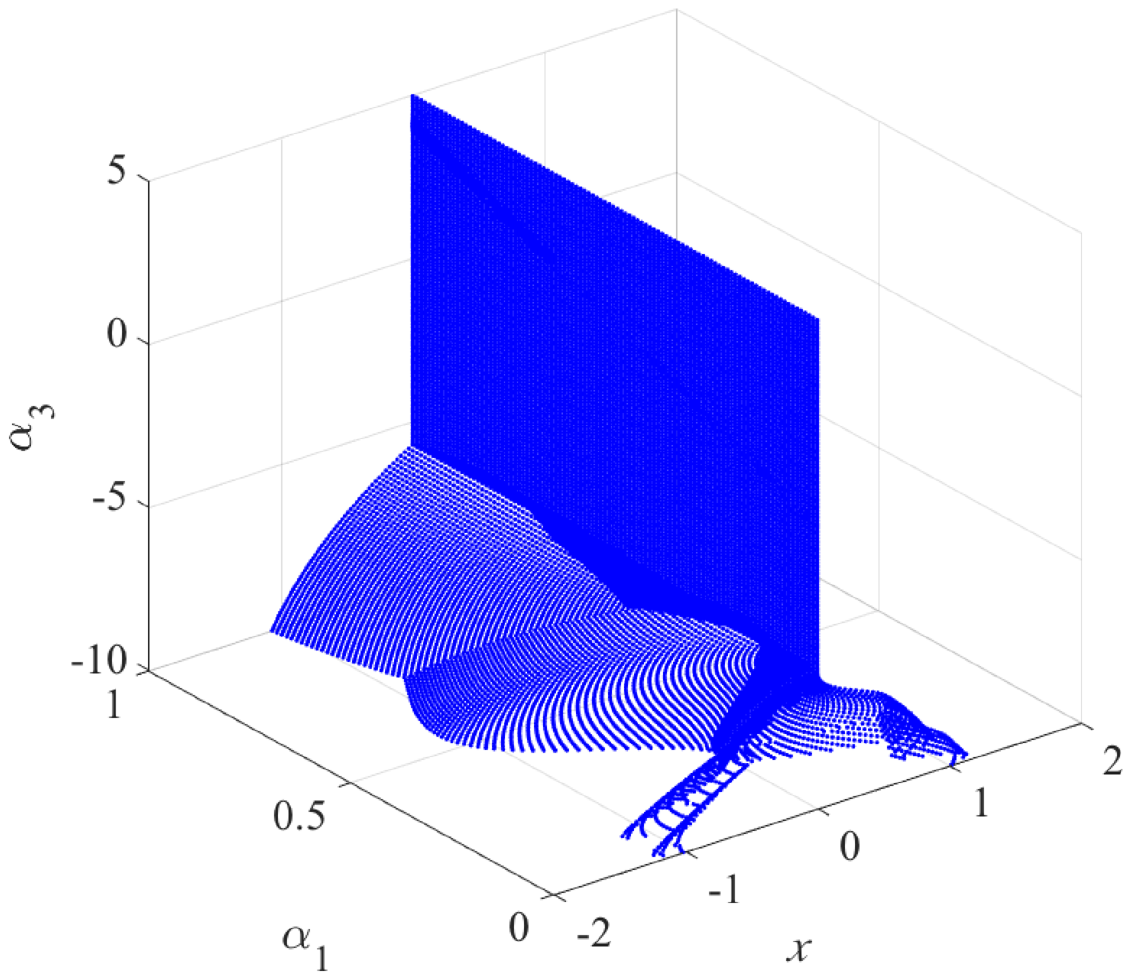

Fig. 5. Bifurcation behaviour of the nonlinear system affected by the parameters α_1 and α_3.

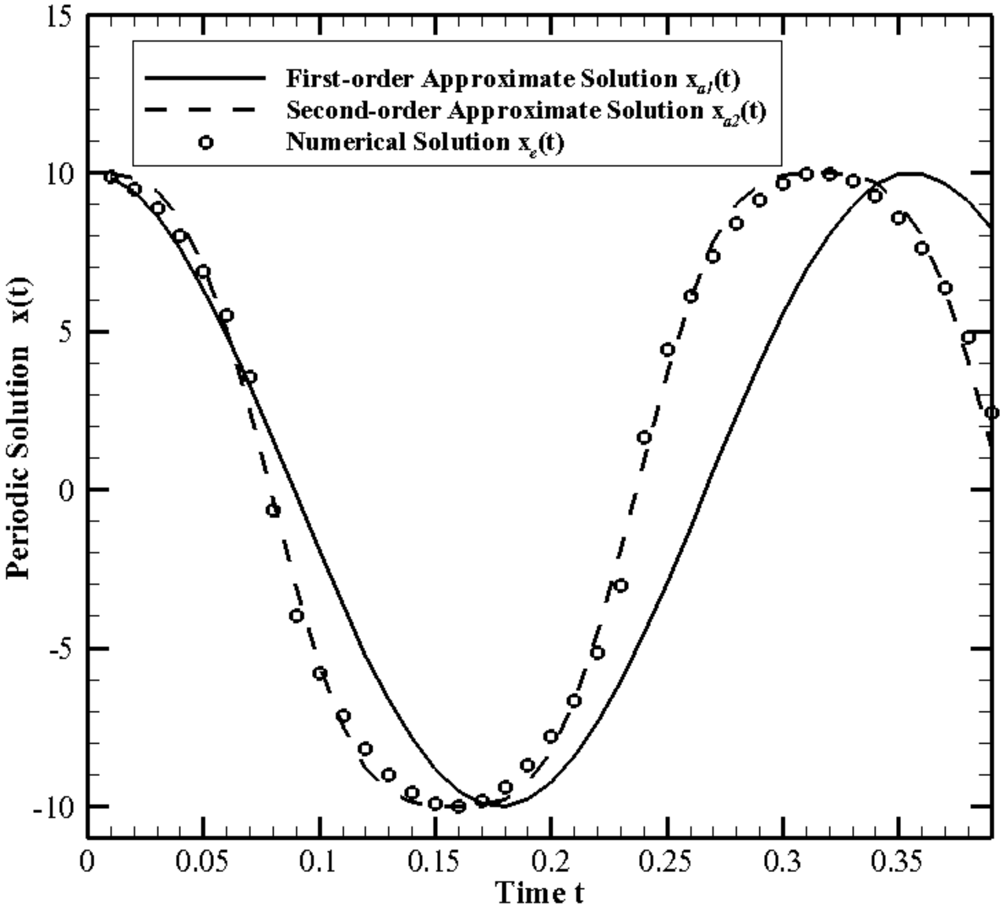

Fig. 6. Comparison of analytical approximate periodic solutions with numerical solution for $\alpha_1 = 0.5$, $\alpha_2 = 2$, $\alpha_3 = -0.2$, $\alpha_4 = 1.3$ and $A = 10$.

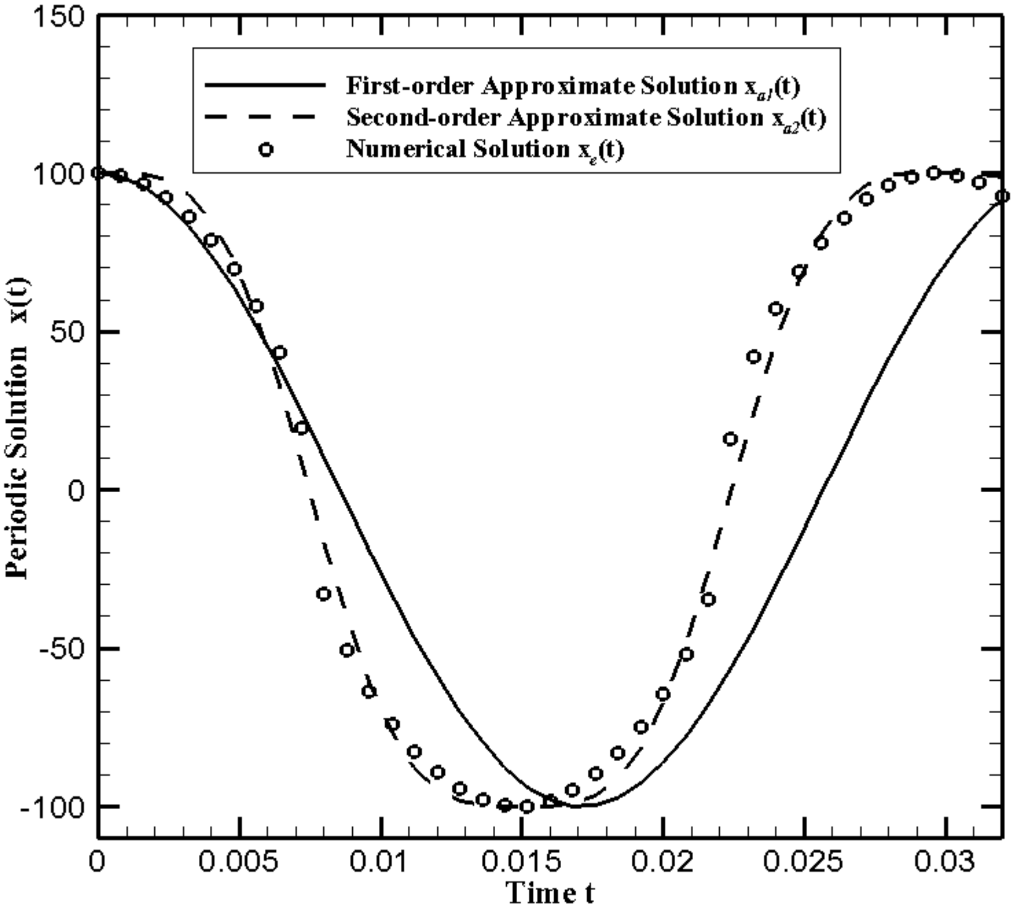

Fig. 7. Comparison of analytical approximate periodic solutions with numerical solution for $\alpha_1 = 0.1$, $\alpha_2 = 1$, $\alpha_3 = -0.5$, $\alpha_4 = 0.27$ **and** $A = 100$.

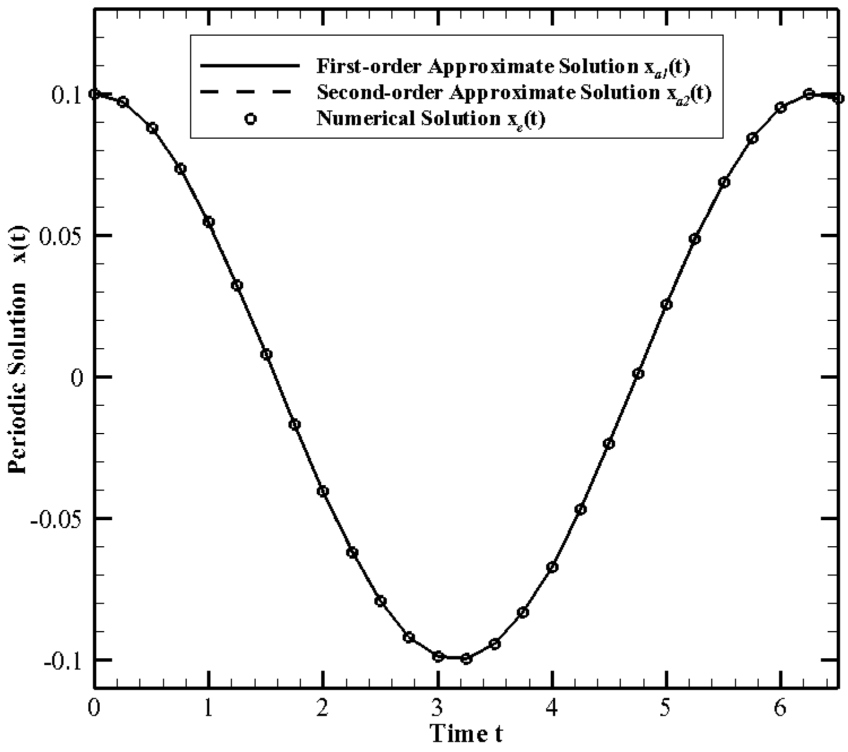

(a)

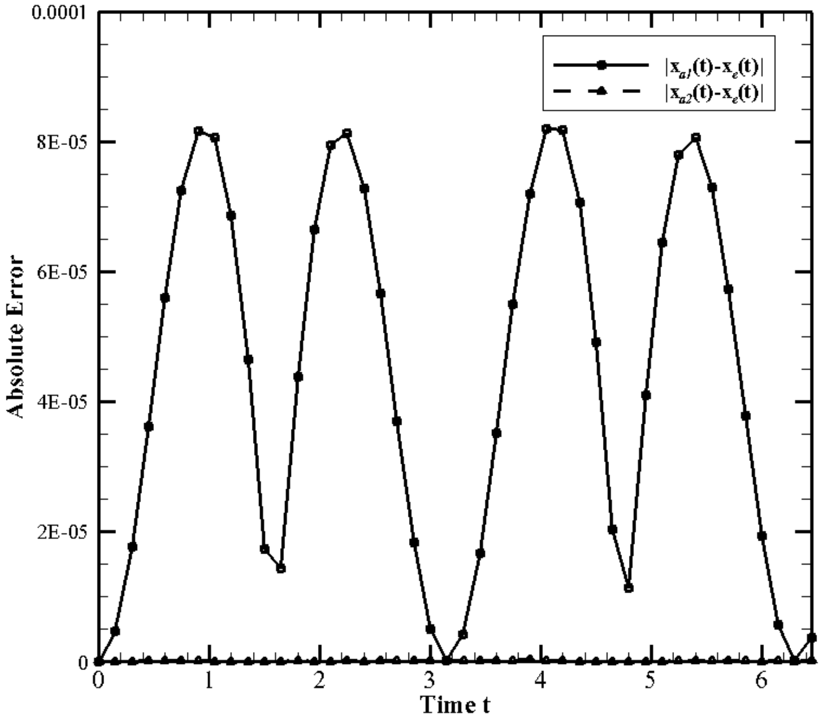

(b)

Fig. 8. (a) Comparison of analytical approximate periodic solutions with numerical solution for $\alpha_1 = 0.1$, $\alpha_2 = 1$, $\alpha_3 = -1.5$, $\alpha_4 = 0.27$ and $A = 0.1$; (b) Comparison of the absolute errors between the approximate and numerical solutions.

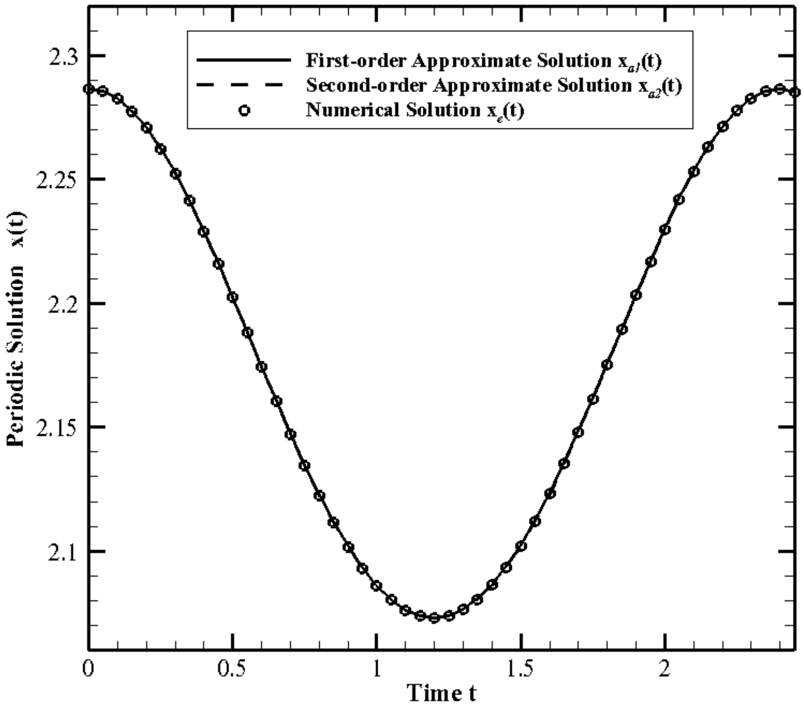

(a)

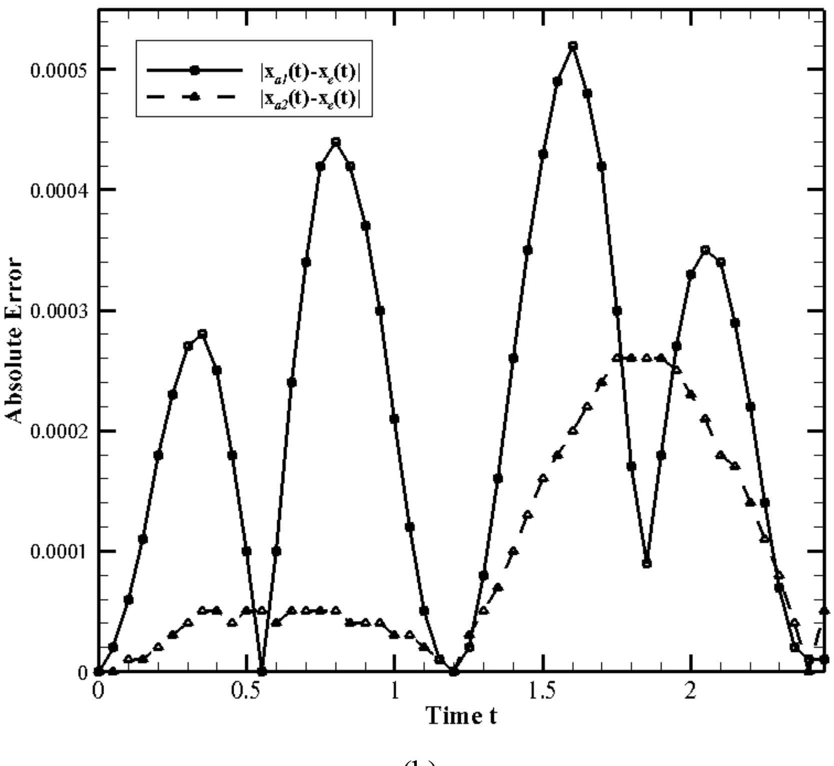

(b)

Fig. 9. (a) Comparison of analytical approximate periodic solutions with numerical solution for $\alpha_1 = 0.1$, $\alpha_2 = 1$, $\alpha_3 = -1.5$, $\alpha_4 = 0.27$ and $A = 2.2865$; (b) Comparison of the absolute errors between the approximate and numerical solutions.

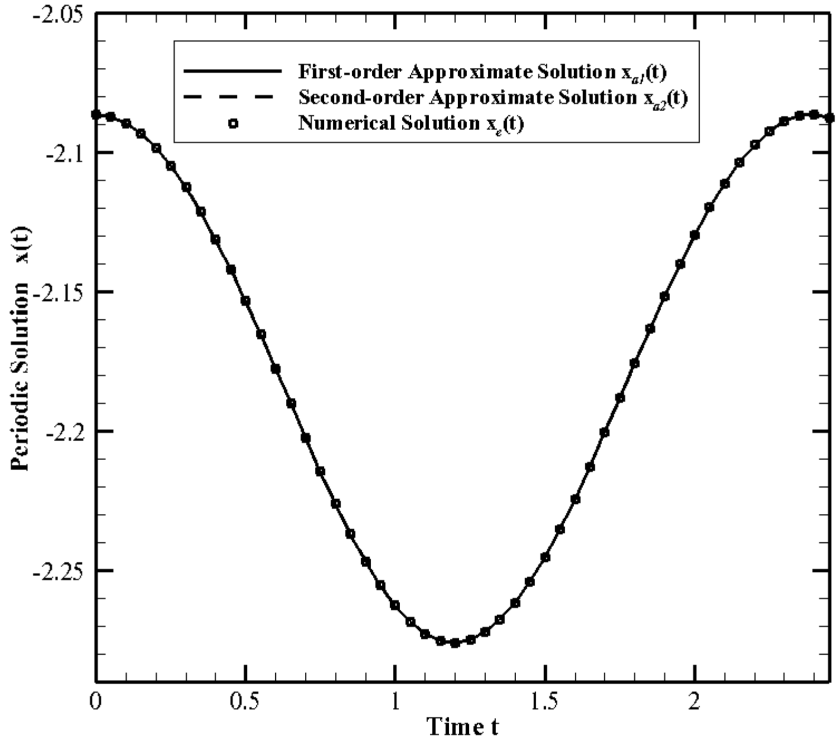

(a)

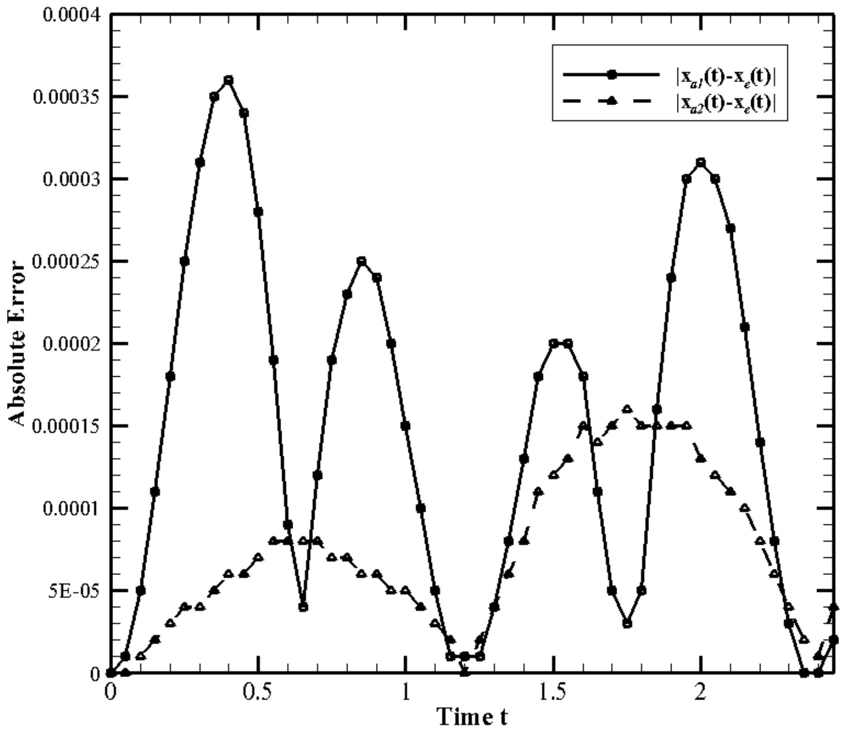

(b)

Fig. 10. (a) Comparison of analytical approximate periodic solutions with numerical solution for $\alpha_1 = 0.1$, $\alpha_2 = 1$, $\alpha_3 = -1.5$, $\alpha_4 = 0.27$ and $A = -2.0865$; (b) Comparison of the absolute errors between the approximate and numerical solutions.